10.1515/astro-2017-0243

Baltic Astronomy, vol. 24, 408–420, 2015

EQUILIBRIUM FIGURES INSIDE THE DARK-MATTER RING AND THE SHAPES OF ELLIPTICAL GALAXIES

B. P. Kondratyev[1,2], N. G. Trubitsyna[3] and E. N. Kireeva[1]

[1] *Sternberg Astronomical Institute, M. V. Lomonosov Moscow State University, 13 Universitetskij prospect, 119992, Russia*

[2] *The Central Astronomical Observatory of the Russian Academy of Sciences at Pulkovo, St. Petersburg, Russia; work@boris-kondratyev.ru*

[3] *Udmurt State University, Izhevsk, Russia*

Received: 2015 November 2; accepted: 2015 November 30

Abstract. We solve the general problem of the theory of equilibrium figures and analyze two classes of liquid rotating gravitating figures residing inside a gravitating ring or torus. These figures form families of sequences of generalized oblate spheroids and triaxial ellipsoids, which at the lower limit of the tidal parameter $\alpha = 0$ have the form of the Maclaurin spheroids and the Jacobi ellipsoids. In intermediate cases $0 < \alpha \leq \alpha_{\max}$ each new sequence of axisymmetric equilibrium figures has two non-rotating boundary spheroids. At the upper limit $\alpha_{\max}/(\pi G\rho) = 0.1867$ the sequence degenerates into a single non-rotating spheroid with the eccentricity $e_{\rm cr} \approx 0.96$ corresponding to the flattening limit of elliptical galaxies (E7). We also perform a detailed study of the sequences of generalized triaxial ellipsoids and find bifurcation points of triaxial ellipsoids in the sequences of generalized spheroids. We use this method to explain the shapes of E-galaxies. According to observations, very slowly rotating oblate E-type galaxies are known that have the shapes, which, because of instability, cannot be supported by velocity dispersion anisotropy exclusively. The hypothesis of a massive dark-matter outer ring requires no extreme anisotropy of pressure; it not only explains the shape of these elliptical galaxies, but also sheds new light on the riddle of the ellipticity limit (E7) of elliptical galaxies.

Key words: celestial mechanics – equilibrium figures – galaxies: elliptical – dark matter

1. INTRODUCTION

One of the main properties of elliptical galaxies is their flattening. Until 1976 the flattening of E-type galaxies was believed to be due to their rotation, and self-consistent analytical models (Gott 1975; Wilson 1975; Larson 1975) were supposed to correctly describe these stellar systems to a first approximation. However, the first measurements (Bertola & Capaccioli 1975; Illingwort 1977) showed actual rotation to be too weak to explain the dynamic oblateness of observed galaxies.

Then the idea of the residual anisotropy of stellar velocity dispersion was proposed (Binney 1978; Kondratyev 1981), which fits well into the general picture of the dynamics of collisionless stellar systems. The riddle of elliptical galaxies has

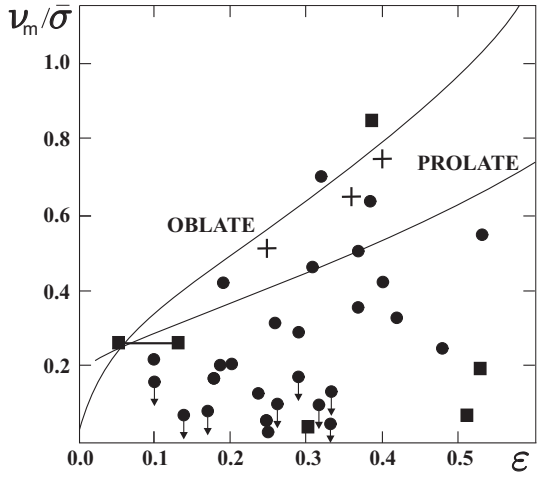

Fig. 1. The $v_{\rm rot}/\sigma$ ratio as a function of oblateness of the elliptical galaxy. The five galaxies marked by the circles with arrows have a significant flattening, but very weak rotation. The figure is adopted from Davies et al. (1983).

stimulated the study of important issues in the theory of collisionless stellar systems. Prominent role was played by two observational tests aimed at determining the spatial shape of E-galaxies (Kondratyev & Ozernoy 1979). One of these tests stated that the sky-plane projection of the rotation axis of triaxial galaxies tends not to coincide with the apparent minor axis of the ellipse. The application of this test soon confirmed that possible geometry of elliptical galaxies indeed includes not only rotationally symmetric shapes like oblate spheroids, but also more complex triaxial ellipsoid figures. It was also established that, unlike liquid configurations, collisionless ellipsoids without internal streams may rotate not just about the minor axis, but also about the middle axis and still remain stable (Kondratyev 1983). However, the challenging problem of the influence of velocity dispersion anisotropy on the stability of three-dimensional collisionless stellar systems is not yet fully explored. The situation is simpler for two-dimensional stellar disks, because they are known to obey the Toomre criterion (Toomre 1984). There is no analogue of such a criterion for E-galaxies, and it remains unclear to what extent they can have prolate velocity ellipsoids and remain stable. Without going into complex details, note that a system with a strong velocity dispersion anisotropy is unstable. For example, spherical stellar systems with purely radial orbits are unstable (Antonov 1973; Polyachenko & Friedman 1976).

In this light, we draw attention to the fact that E-galaxies with very weak rotation and large oblateness have been observed (Davies et al. 1983) (see Fig. 1).

The question naturally arises: what factor can in the absence of rotation maintain the shape of E-galaxies?

In this paper, we propose a different approach to explaining the equilibrium shape of elliptical galaxies. We formulate and solve the general problem of equilibrium figures inside a dark-matter ring. We already studied equilibrium figures inside the ring and torus in our earlier paper (Kondratyev & Trubitsyna 2010). Here we further develop and modify our method, which provides a new insight

into interpreting the riddle of marginal flattening of E-galaxies. We also study in detail the sequences of generalized triaxial ellipsoids and find bifurcation points in the sequences of triaxial ellipsoids of generalized spheroids.

2. FORMULATION OF THE PROBLEM AND EQUILIBRIUM EQUATIONS

Consider an equilibrium figure of rotating liquid gravitating mass with the shape of an oblate spheroid or triaxial ellipsoid located inside a gravitating ring or torus. The figure rotates about the Ox_3 axis with angular velocity Ω, and its equatorial plane coincides with the coordinate plane Ox_1x_2. Let us find the equilibrium conditions for such a figure. The potential of a homogeneous ellipsoid at an interior point (x_1, x_2, x_3) is given by the following well-known formula (Chandrasekhar 1969):

$$\varphi = \pi G\rho \left(I - A_1 x_1^2 - A_2 x_2^2 - A_3 x_3^2\right), \tag{1}$$

where

$$\begin{aligned} &I = a_1a_2a_3 \int\limits_0^\infty \frac{ds}{\Delta(s)};\ \Delta(s) = \sqrt{(a_1^2+s)(a_2^2+s)(a_2^2+s)};\\ &A_1 = a_1a_2a_3 \int\limits_0^\infty \frac{ds}{(a_1^2+s)\Delta(s)};\ A_2 = a_1a_2a_3 \int\limits_0^\infty \frac{ds}{(a_2^2+s)\Delta(s)};\\ &A_3 = a_1a_2a_3 \int\limits_0^\infty \frac{ds}{(a_3^2+s)\Delta(s)}. \end{aligned} \tag{2}$$

We further restrict our analysis to the tidal influence of the gravitational field of a ring or torus. It can be shown that in the tidal approximation the potential of any ring can be in the general case written as (Kondratyev & Trubitsyna 2010)

$$\varphi_{\text{ring}}(x_1, x_2, x_3) = \alpha\left(x_1^2 + x_2^2 - 2x_3^2\right),\ \alpha > 0 \tag{3}$$

with non-negative constant α. It is important that formula (3) provides a universal representation of tidal potential, and below we describe an elegant method for determining the constant α for each particular model of a ring or torus.

Given the centrifugal potential, the full potential at any interior point, including the surface of figure, can be written as

$$\Phi(x_1, x_2, x_3) = \varphi(x_1, x_2, x_3) + \frac{\Omega^2}{2}\left(x_1^2 + x_2^2\right) + \alpha\left(x_1^2 + x_2^2 - 2x_3^2\right). \tag{4}$$

After rearranging the terms in formula (4) we have a quadratic form in the coordinates (x_1, x_2, x_3):

$$\begin{aligned} \Phi(x_1, x_2, x_3) = &\left(-\pi G\rho A_1 + \frac{\Omega^2}{2} + \alpha\right) x_1^2 + \left(-\pi G\rho A_2 + \frac{\Omega^2}{2} + \alpha\right) x_2^2 - \\ &- \left(\pi G\rho A_3 + 2\alpha\right) x_3^2. \end{aligned} \tag{5}$$

According to the theory of equilibrium figures (Subbotin 1949; Kondratyev 1989), the rotating liquid mass is in a state of relative equilibrium if its surface coincides with an equipotential surface $\Phi = \text{const}$. According to this fundamental principle, the following condition of proportionality should be satisfied:

$$\left(-\pi G\rho A_1 + \frac{\Omega^2}{2} + \alpha\right) x_1^2 + \left(-\pi G\rho A_2 + \frac{\Omega^2}{2} + \alpha\right) x_2^2 - \left(\pi G\rho A_3 + 2\alpha\right) x_3^2 = \\ = \kappa \left(\frac{x_1^2}{a_1^2} + \frac{x_2^2}{a_2^2} + \frac{x_3^2}{a_3^2}\right) \tag{6}$$

(κ is the proportionality factor). Condition (6) yields the proportion

$$\left(\frac{\Omega^2}{2\pi G\rho} - A_1 + \frac{\alpha}{\pi G\rho}\right) a_1^2 = \left(\frac{\Omega^2}{2\pi G\rho} - A_2 + \frac{\alpha}{\pi G\rho}\right) a_2^2 = -\left(A_3 + \frac{2\alpha}{\pi G\rho}\right) a_3^2 . \tag{7}$$

Here we have two basic equations of relative equilibrium for liquid gravitating figures. We use them as follows.

First, we determine from Eq. (7) the angular velocity Ω:

$$\begin{aligned} \frac{\Omega^2}{2\pi G\rho} &= A_1 - \frac{a_3^2}{a_1^2} A_3 - \frac{\alpha}{\pi G\rho}\left(1 + 2\frac{a_3^2}{a_1^2}\right); \\ \frac{\Omega^2}{2\pi G\rho} &= A_2 - \frac{a_3^2}{a_2^2} A_3 - \frac{\alpha}{\pi G\rho}\left(1 + 2\frac{a_3^2}{a_2^2}\right); \\ \frac{\Omega^2}{2\pi G\rho} &= \frac{A_1 a_1^2 - A_2 a_2^2}{a_1^2 - a_2^2} - \frac{\alpha}{\pi G\rho} . \end{aligned} \tag{8}$$

We eliminate Ω^2 from the first two relations of Eq. (8) to obtain the following equation linking the semi-axes of the equilibrium ellipsoid:

$$A_1 - A_2 + A_3 a_3^2 \left(\frac{1}{a_2^2} - \frac{1}{a_1^2}\right) + \frac{2\alpha}{\pi G\rho} a_3^2 \left(\frac{1}{a_2^2} - \frac{1}{a_1^2}\right) = 0 . \tag{9}$$

We write the difference between the coefficients $A_1 - A_2$ in (9) using integral index A_{12}:

$$A_1 - A_2 = -\left(a_1^2 - a_2^2\right) a_1 a_2 a_3 \int_0^\infty \frac{ds}{\left(a_1^2 + s\right)\left(a_2^2 + s\right)\Delta(s)} = -\left(a_1^2 - a_2^2\right) A_{12} . \tag{10}$$

Equation (9) can then be written in a concise form

$$\left(a_1^2 - a_2^2\right)\left[-A_{12} + A_3 \frac{a_3^2}{a_1^2 a_2^2} + \frac{2\alpha}{\pi G\rho} \cdot \frac{a_3^2}{a_1^2 a_2^2}\right] = 0 . \tag{11}$$

In Eqs. (8) and (11) we have two variants of the equilibrium figures:

First option. The homogeneous liquid gravitating mass has the form of an axisymmetric oblate spheroid

$$a_1 = a_2 \le a_3 , \tag{12}$$

which rotates in accordance with any of the first two equations (8), with angular velocity

$$\frac{\Omega^2}{2\pi G\rho} = A_1 - \frac{a_3^2}{a_1^2}A_3 - \frac{\alpha}{\pi G\rho}\left(1 + \frac{2a_3^2}{a_1^2}\right). \tag{13}$$

Second option. If $a_1 \neq a_2$, then the equilibrium figure is a triaxial ellipsoid and its geometric shape for the given parameter α is given by the following equation:

$$-A_{12} + A_3\frac{a_3^2}{a_1^2a_2^2} + \frac{2\alpha}{\pi G\rho}\frac{a_3^2}{a_1^2a_2^2} = 0\,. \tag{14}$$

Equation (14) links implicitly the two independent relationships of semiaxes of the ellipsoid, for example, a_3/a_1 and a_2/a_1. The angular velocity of triaxial equilibrium figures follows from the third equation (8):

$$\frac{\Omega^2}{2\pi G\rho} = \frac{A_1a_1^2 - A_2a_2^2}{a_1^2 - a_2^2} - \frac{\alpha}{\pi G\rho}\,. \tag{15}$$

In the particular case where the outer ring is absent, $\alpha = 0$, and Eq. (13) becomes the well-known formula for the angular velocity of Maclaurin spheroids,

$$\frac{\Omega^2}{2\pi G\rho} = A_1 - \frac{a_3^2}{a_1^2}A_3\,, \tag{16}$$

and from (14) and (15) follow two formulas,

$$\begin{aligned} a_1^2a_2^2A_{12} &= A_3a_3^2\,,\\ \frac{\Omega^2{}_{\text{Jacobi}}}{2\pi G\rho} &= \frac{A_1a_1^2 - A_2a_2^2}{a_1^2 - a_2^2}\,, \end{aligned} \tag{17}$$

which describe the shape and the angular velocity of classical triaxial Jacobi ellipsoids.

However, if $\alpha \neq 0$, then equations (13), (14) and (15) define two new classes of equilibrium figures. We call them generalized spheroids and generalized triaxial ellipsoids. These new equilibrium figures should be studied separately.

3. SPHEROIDAL EQUILIBRIUM FIGURES

If $a_1 = a_2$, we have a two-parameter family of generalized spheroidal equilibrium figures whose rotation is described by the formula

$$\frac{\Omega^2(e)}{2\pi G\rho} = \frac{\Omega_0^2(e)}{2\pi G\rho} - \frac{\alpha}{\pi G\rho}\left(3 - 2e^2\right), \tag{18}$$

where, according to Eq. (13),

$$\frac{\Omega_0^2(e)}{2\pi G\rho} = \frac{\sqrt{1-e^2}}{e^3}\left(3 - 2e^2\right)\arcsin e - \frac{3}{e^2}\left(1 - e^2\right), \quad e \equiv\ e_{13} = \sqrt{1 - a_3^2/a_1^2} \tag{19}$$

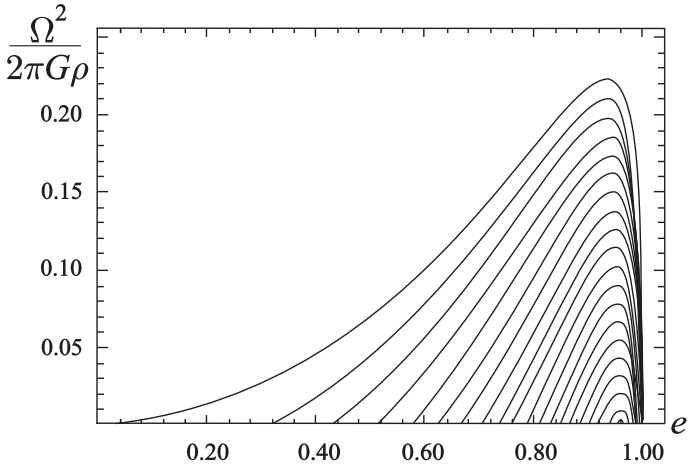

Fig. 2. Squared angular velocity (in $2\pi G\rho$ units) as a function of eccentricity for the family of generalized fixed-α sequences of spheroids. The upper curve shows the eccentricity dependence for $\alpha = 0$ (no ring). The curves below it show the corresponding dependences for fixed α values increasing in 0.01 increments. The curve for $\alpha = \alpha_{\max}$ degenerates to a point. The $\alpha_{\max}$ and $e_{\rm cr}$ values are given in the text.

is the normalized squared angular velocity of classical Maclaurin spheroids. Here we took into account the well-known formulas (Chandrasekhar 1969) for the coefficients $A_1(e)$ and $A_3(e)$ for internal potential of oblate spheroid:

$$\begin{aligned} A_1 = A_2 &= \frac{\sqrt{1-e^2}}{e^3}\arcsin e - \frac{1-e^2}{e^2}, \\ A_3 &= \frac{2}{e^2} - 2\frac{\sqrt{1-e^2}}{e^3}\arcsin e\,. \end{aligned} \tag{20}$$

Formula (18) can be presented in graphical form (Fig. 2).

Each sequence corresponds to a particular fixed α; if $\alpha = 0$ (no ring), we have a sequence of the Maclaurin spheroids. The curves for sequences with $\alpha > 0$ lie below the Maclaurin curve. These curves degenerate to a point at $\alpha = \alpha_{\max}$. The critical values $\alpha_{\max}$ and $e_{\rm cr}$ can be found from the following equations:

$$\begin{aligned} &\frac{\alpha}{\pi G\rho}\left(3-2e^2\right) = \frac{\Omega_0^2(e)}{2\pi G\rho}, \\ &\frac{d}{de}\Omega^2(e) = 0 \quad \rightarrow \quad \frac{d}{de}\frac{\Omega_0^2(e)}{2\pi G\rho} + 4e\frac{\alpha}{\pi G\rho} = 0\,, \end{aligned} \tag{21}$$

or, in expanded form,

$$\begin{aligned} &\frac{\sqrt{1-e^2}\left(3-2e^2\right)\arcsin e}{e^3} - \frac{3\left(1-e^2\right)}{e^2} - \frac{\alpha}{\pi G\rho}\left(3-2e^2\right) = 0\,, \\ &\frac{9-2e^2}{e^3} - \frac{9-8e^2}{e^4\sqrt{1-e^2}}\arcsin e + 4\frac{\alpha}{\pi G\rho}e = 0\,. \end{aligned} \tag{22}$$

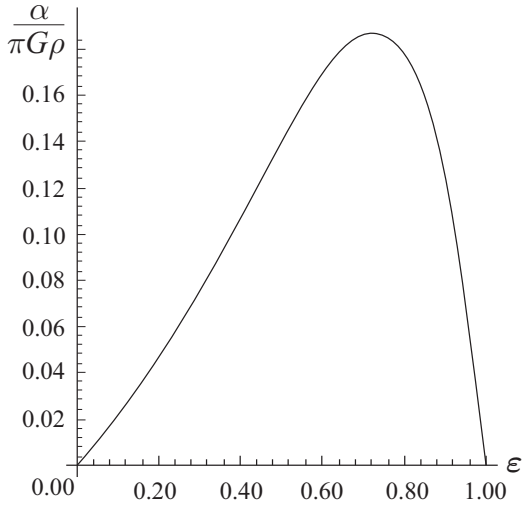

Fig. 3. Normalized parameter $\alpha/(\pi G\rho)$ as a function of the ellipticity of the spheroid with the shape sustained by its own gravity and the gravity of the outer dark-matter ring. The maximum $\alpha_{\max}/(\pi G\rho) \approx 0.1867$ separates the planetary and disk spheroid figures.

We eliminate α from both equations (22) to obtain, after some rearrangements, the following implicit equation for the critical eccentricity $e_{\rm cr}$ of the spheroid:

$$\frac{3}{e^3} + \frac{4e}{\left(3-2e^2\right)^2} - \frac{\left(3-2e^2\right)\arcsin e}{e^4\sqrt{1-e^2}} = 0\,. \tag{23}$$

We solve equation (23) numerically to find

$$e_{\rm cr} = 0.9600029518. \tag{24}$$

The corresponding limit value $\alpha_{\max}$ is

$$\frac{\alpha_{\max}}{\pi G\rho} = 0.1866928655. \tag{25}$$

We show the first equation in (21) in graphic form in Fig. 3.

Note that for each $\alpha/(\pi G\rho)$ value from the interval found in Eq. (26) there are two associated spheroidal equilibrium figures. Note, however, there is only one figure associated with the critical value of the parameter $\alpha/(\pi G\rho) \approx 0.1867$. Here we study only the planetoid branch that begins with a sphere and ends with an E7 spheroid.

Thus, axisymmetric figures inside a ring, which are considered here, are represented by a family of sequences of generalized spheroids. For each α value in the interval

$$0 \le \alpha \le \alpha_{\max} = \pi G\rho \cdot 0.1866928655 \tag{26}$$

there is the corresponding sequence of equilibrium spheroids with oblateness in the interval

$$e_{\min}(\alpha) \le e \le e_{\max}(\alpha)\,. \tag{27}$$

The minimum and maximum oblateness, $e_{\min}(\alpha)$ and $e_{\max}(\alpha)$, can be found from the following implicit equation:

$$\frac{\Omega_0^2(e)}{2\pi G\rho} = \frac{\alpha}{\pi G\rho}\left(3 - 2e^2\right). \tag{28}$$

The series of equilibrium figures corresponding to $\alpha = 0$ (the Maclaurin spheroids) begins with a sphere and ends with a flat disc. At $\alpha < \alpha_{\rm cr}$, each sequence has two non-rotating spheroids (the first and the last ones). At $\alpha = \alpha_{\rm cr}$, the sequence of figures degenerates into a single non-rotating spheroid with the eccentricity equal to $e_{\rm cr} = 0.9600029518$.

4. LIMITING DEGREE OF VELOCITY DISPERSION ANISOTROPY IN E7-TYPE GALAXIES

As is well known (Kondratyev 1982, 2003), the rotational energy of gravitating configurations in inertial reference frame is given by the formula

$$T_{\rm rot} = \frac{1}{2}\left(2kW_{33} - W_{11} - W_{22}\right), \tag{29}$$

where W_{ij} are components of the gravitational energy tensor of the body,

$$W_{ij} = \int\limits_V \rho(x)\,\varphi_{ij}(x)\,dV, \tag{30}$$

$\rho(x)$ is the density, and

$$\varphi_{ij}(x) = G\int\limits_V \rho(x)\,\frac{(x_i - x'_i)\,(x_j - x'_j)}{|x - x'|^3}dV' \tag{31}$$

is the tensor potential of the body at sampling point x. The coefficient in the formula (29)

$$k = \frac{\Pi_{11} + \Pi_{22}}{2\Pi_{33}} \tag{32}$$

can be written in terms of components of the tensor energy of chaotic motion of stars,

$$\Pi_{ij} = \int\limits_V \rho(x)\,(\dot{x}_i - u_i)\,(\dot{x}_j - u_j)dV. \tag{33}$$

The coefficient k is a measure of velocity dispersion anisotropy: $k = 1$ for systems with isotropic pressure, but the converse is not true, because $k = 1$ does not rule out $\Pi_{11} \neq \Pi_{22}$.

For numerical estimates we consider the case of axisymmetric stellar system $\Pi_{11} = \Pi_{22}$. The anisotropy factor then is

$$k = \frac{\Pi_{11}}{\Pi_{33}} = \frac{\sigma_{11}^2}{\sigma_{33}^2}. \tag{34}$$

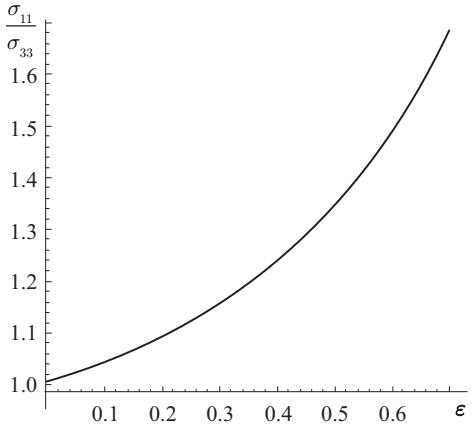

Fig. 4. Dependence of the velocity dispersion anisotropy σ_{11}/σ_{33} on the ellipticity $\varepsilon = 1 - \sqrt{1-e^2}$ for spheroidal equilibrium figures. The $\varepsilon \approx 0.7$ value corresponds to the elliptical galaxy with the limiting oblateness E7.

It is important that (Kondratyev 1982, 2003) the rotational-to-gravitational energy ratio in heterogeneous ellipsoids (spheroids) consisting of similar equidensity layers does not depend on the concentration of matter in them, and coincides exactly with the corresponding ratio of the classical homogeneous equilibrium figures. For spheroids this ratio is equal to

$$t\,(e) = \frac{T_{\rm rot}}{|W|} = \frac{3}{2e^2} - 1 - \frac{3\sqrt{1-e^2}}{2e\arcsin e} \tag{35}$$

and is a function of the eccentricity layer exclusively.

It follows from formula (29) that

$$k = \frac{a_1^2 A_1}{a_3^2 A_3}. \tag{36}$$

The formulas for A_1 and A_3 are given in Eq. (20). In view of Eq. (34), we now find the unknown ratio of the stellar velocity dispersion in the equatorial plane of the spheroid to the velocity dispersion in the direction of the Ox_3 axis to be

$$\frac{\sigma_{11}}{\sigma_{33}} = \sqrt{k} = \sqrt{\frac{a_1^2 A_1}{a_3^2 A_3}}. \tag{37}$$

We plot function (37) in Fig. 4.

We see that anisotropy for E7-type galaxies reaches $\sigma_{11}/\sigma_{33} = 1.7$. Stellar spheroids with such large anisotropy should be unstable.

5. ELLIPSOIDAL EQUILIBRIUM FIGURES

Consider another case $a_1 \neq a_2$. The angular velocity of the generalized triaxial ellipsoids is equal to

$$\frac{\Omega^2}{2\pi G\rho} = \frac{\Omega^2{}_{\rm Jacobi}}{2\pi G\rho} - \frac{\alpha}{\pi G\rho}, \tag{38}$$

where ${\Omega^2}_{\rm Jacobi}/(2\pi G\rho)$ is the squared normalized angular velocity of the Jacobi ellipsoids from Eqs. (17).

It is important to investigate the relationship between the known generalized spheroids and triaxial figures. First, in the limit $a_1 \to a_2$ the ellipsoid turns into spheroid. Formula (38) then gives

$$\frac{\Omega^2\,(e)}{2\pi G\rho} = B_{11} - \frac{\alpha}{\pi G\rho}\,. \tag{39}$$

This spheroid also belongs to a sequence of generalized spheroids with an appropriate $\alpha/(\pi G\rho)$ and rotates with angular velocity

$$\frac{\Omega^2(e)}{2\pi G\rho} = e^2 B_{13} - \frac{\alpha}{\pi G\rho}\left(3 - 2e^2\right). \tag{40}$$

We now equate the right-hand sides in equations (39) and (40) to obtain

$$e^2 B_{13} - B_{11} = \frac{2\alpha}{\pi G\rho}\left(1 - e^2\right), \tag{41}$$

or

$$a^4 A_{11} - a_3^2\left(a_1^2 - a_3^2\right) A_{13} - a_3^2 A_1 = \frac{2\alpha}{\pi G\rho}\,, \tag{42}$$

where

$$\begin{aligned}
A_{11} &= a_1^2 a_3 \int\limits_0^\infty \frac{ds}{\left(a_1^2+s\right)^4\sqrt{a_3^2+s}} = \\
&= a_1^2 a_3 \frac{1}{48}\left(16a_3^5\sqrt{a_1^2-a_3^2} + 30\arctan\left(\frac{a_3}{\sqrt{a_1^2-a_3^2}}\right)\cdot a_1^6 - \right. \\
&\left. -52a_3^3a_1^2\sqrt{a_1^2-a_3^2} + 66a_3a_1^4\sqrt{a_1^2-a_3^2} - 15\pi a_1^6\right) \Bigg/ \left(a_1^6\sqrt{a_1^2-a_3^2}\left(a_3^2-a_1^2\right)^3\right); \\
A_{13} &= a_1^2 a_3 \int\limits_0^\infty \frac{ds}{\left(a_1^2+s\right)^2\left(a_3^2+s\right)^{\frac{3}{2}}} = \frac{a_1^2 a_3}{2}\left(4\sqrt{a_1^2-a_3^2}\cdot a_1^2 + 2a_3^2\sqrt{a_1^2-a_3^2} + \right. \\
&\left. +6\arctan\left(\frac{a_3}{\sqrt{a_1^2-a_3^2}}\right) a_3a_1^2 - 3\pi a_1^2 a_3\right) \Bigg/ \left(a_1^2a_3\sqrt{a_1^2-a_3^2}\left(a_1^2-a_3^2\right)^2\right).
\end{aligned} \tag{43}$$

We plot in Fig. 5 the eccentricity dependences of squared angular velocity for generalized spheroids and the corresponding dependences for the sequences of triaxial ellipsoids bifurcating from these spheroids.

The shape of triaxial ellipsoids is defined by two independent semiaxial ratios a_3/a_1, a_2/a_1, and can be described by complicated implicit equation (14). The following substitutions

$$\lambda = \frac{a_3}{a_1}, \quad \mu = \frac{a_3}{a_2}, \quad \nu = \frac{\lambda}{\mu} = \frac{a_2}{a_1}, \quad s = a_3^2 u \tag{44}$$

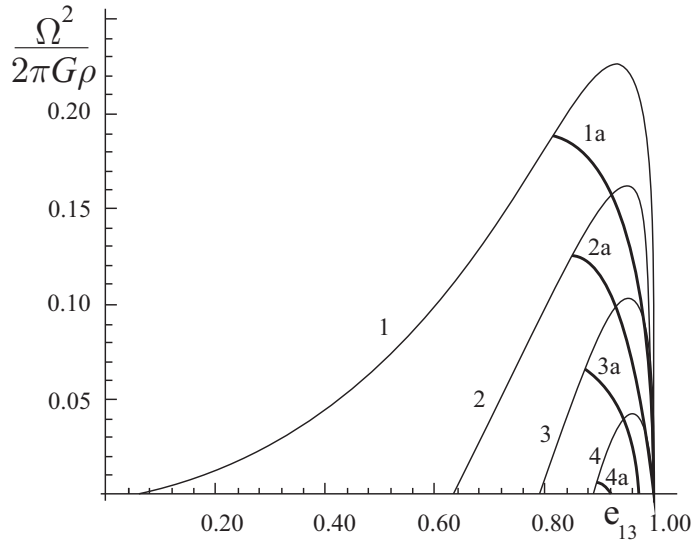

Fig. 5. Eccentricity dependence of the squared angular velocity (in the units of $2\pi G\rho$) along the sequences of generalized spheroids (curves 1,2,3,4) and along the sequences of generalized triaxial ellipsoids bifurcating from it (curves $1_a, 2_a, 3_a, 4_a$). Each sequence of spheroids and sequence of ellipsoids bifurcating from them is characterized by a particular fixed parameter $\alpha/(\pi G\rho)$; $\alpha = 0$ for the top curve (no ring), which corresponds to the Maclaurin spheroids and the Jacobi ellipsoids. The curves below it are for $\alpha/(\pi G\rho) = 0.05;\ 0.10;\ 0.15$.

transform equation (14) into

$$\int_0^\infty \frac{u\left(1-\lambda^2-\mu^2\right)-1}{(1+\lambda^2 u)^{3/2}(1+\mu^2 u)^{3/2}(1+u)^{3/2}}du = \frac{2\alpha}{\pi G\rho}\,. \tag{45}$$

Equation (45) defines a family of sequences of generalized triaxial ellipsoids. For numerical calculations this equation can be conveniently reduced to the following form:

$$\begin{aligned}
&\mu\frac{\lambda^2\left(1-\mu^2\right)^3+\mu^2\left(1-\lambda^2\right)^3+\left(1-\lambda^2\right)^{\frac{3}{2}}\sqrt{\mu^2-\lambda^2}\left(2-\lambda^2-\mu^2\right)}{\left(1-\lambda^2\right)^{\frac{3}{2}}\left(1-\mu^2\right)^2\left(\mu^2-\lambda^2\right)^2}\times\\
&\times E\left(\sqrt{1-\lambda^2},\sqrt{\frac{1-\nu^2}{1-\lambda^2}}\right)-\\
&-\frac{\lambda^2\mu\left(2-2\lambda^2-2\mu^2+\lambda^4+\mu^4\right)}{\left(1-\lambda^2\right)^{\frac{3}{2}}\left(1-\mu^2\right)\left(\mu^2-\lambda^2\right)^2}F\left(\sqrt{1-\lambda^2},\sqrt{\frac{1-\nu^2}{1-\lambda^2}}\right)+\\
&-\frac{\left(2-\lambda^2-\mu^2\right)\left(\mu^2-\lambda^2\right)+\mu^2\left(1-\lambda^2\right)^2}{\left(1-\lambda^2\right)\left(1-\mu^2\right)^2\left(\mu^2-\lambda^2\right)}=\frac{\alpha}{\pi G\rho},
\end{aligned} \tag{46}$$

which includes incomplete elliptic integrals of the first and second kind.

6. DISCUSSION

The presence of dark matter both inside galaxies and in the surrounding halos has been debated extensively in the literature. Dynamically, dark matter behaves like ordinary baryonic matter and can therefore likewise form ring structures. According to current data, the amount of dark matter in the Universe significantly (by one and a half orders of magnitude) exceeds that of baryonic matter, and hence outer rings around galaxies may have huge masses. The mass of such a ring can be estimated by the formula which links the tidal parameter α to the mass of the external torus, M_1 (Kondratyev & Trubitsyna 2010):

$$\alpha = \frac{M_1 G}{3\pi r_0} \frac{1}{k R_0^2} \left[\left(1 - k^2\right) K\left(k\right) - \left(1 - 2k^2\right) E\left(k\right) \right]. \tag{47}$$

Here, r_0 is the radius of the torus pipe; R_0, the radius of its center line; ρ_1, the density of dark matter, and $k = r_0/R_0$, the parameter of the complete elliptic integral. We adopt the following estimates,

$$\frac{\alpha}{\pi G \rho_1} = 0.1, \;\; R_0 = 20 \text{ kpc}, \;\; k = 0.05, \;\; \rho_1 = 2 \cdot 10^{-30} \text{ g cm}^{-3}, \tag{48}$$

to derive from (47) the mass of the outer dark-matter torus

$$M_1 \sim 4 \cdot 10^{12} M_\odot. \tag{49}$$

Thus, to sustain the critical oblateness of an average elliptical galaxy, the outer ring should be about one order of magnitude more massive than that of the galaxy. This conclusion is consistent with the known dark-to-baryonic mass ratio in the Universe.

This study analyzes two classes of rotating liquid equilibrium figures residing inside a gravitating ring or torus. These figures form families of sequences of generalized oblate spheroids and triaxial ellipsoids. For any value of the tidal parameter α in the interval $0 \leq \alpha/(\pi G\rho) \leq 0.1867$ there is an associated sequence of the spheroids or ellipsoids of a new type with eccentricities in the range $e_{\min}(\alpha) \leq e \leq e_{\max}(\alpha)$. Interestingly, small angular velocity does not imply that the corresponding generalized spheroids differ little from a sphere. Indeed, if $0 < \alpha \leq \alpha_{\max}$, then each sequence of equilibrium figures is bounded by two generalized non-rotating spheroids with different ellipticity. This study also includes a detailed analysis of generalized triaxial ellipsoids including the computation of the bifurcation points of triaxial ellipsoids from the sequences of the generalized spheroids.

At the upper limit $\alpha = \alpha_{\max}$, the sequence degenerates into a single oblate non-rotating spheroid with the eccentricity $e_{\text{cr}} \approx 0.9600$ which corresponds to the limit flattening of elliptical galaxies E7. It is shown that the equilibrium of the flattened isolated galaxies without rotation is unstable and cannot be maintained only by the anisotropy of the velocity dispersion of stars. To create noticeable flattening of the galaxy, the mass of the ring should be approximately an order of magnitude greater than that of the galaxy, which is consistent with the known mass ratio of dark and baryonic matter in the Universe. The ring stabilizes the galaxy and is an important complement to the dynamical models of isolated galaxies. The effect of a massive outer ring can shed light on the mystery of the existence of galaxies with a critical flattening E7.

REFERENCES

Antonov V. A. 1973, Sov. Astron., 17, 428
Bertola F., Capassioli M. 1975, ApJ, 200, 439
Binney J. J. 1978, MNRAS, 183, 501
Chandrasekhar S. 1969, *Ellipsoidal Figures of Equilibrium*, Yale University Press, New Haven and London
Davies R. L., Efstathiou G., Fall S. M., Illingworth G., Schechter P. L. 1983, ApJ, 266, 41
Gott I. R. 1975, ApJ., 201, 296
Illingworth G. 1977, ApJ, 218, L43
Kondratyev B. P. 1981, Sov. Astron. Lett., 7, 45
Kondratyev B. P. 1982, Sov. Astron., 59, 458
Kondratyev B. P. 1983, Sov. Astron., 27, 497
Kondratyev B. P., 1989, *Dynamics of Gravitating Ellipsoidal Figures*, Nauka, Moscow
Kondratyev B. P., 2003, *The Potential Theory and Equilibrium Figures*, RHD, Moscow-Izhevsk
Kondratyev B. P., Ozernoy L. M. 1979, Sov. Astron. Lett, 5, 37
Kondratyev B. P., Trubitsyna N. G. 2010, Astrophysics, 53, 189
Larson R. B. 1975, MNRAS, 173, 671
Polyachenko V. L., Friedman, A. M., 1976, *Equilibrium and Stability of Gravitating Systems*, Nauka, Moscow
Subbotin M. F. 1949, *Course in Celestial Mechanics*, 3, GITTL, Leningrad – Moscow
Toomre A. 1984, ApJ, 139, 1217
Wilson C. P. 1975, AJ, 80, 175